THE UNIVERSITY *of* EDINBURGH

Edinburgh Research Explorer

Measurement of Z -> tau(+)tau(-) production in proton-proton collisions at root s=8 TeV

OPEN ACCESS

Measurement of $Z \to \tau^+\tau^-$ production in proton-proton collisions at $\sqrt{s} = 8\,\text{TeV}$

JHEP09(2018)159

The LHCb collaboration

E-mail: chitsanu.khurewathanakul@cern.ch

ABSTRACT: A measurement of $Z \to \tau^+\tau^-$ production cross-section is presented using data, corresponding to an integrated luminosity of $2\,\text{fb}^{-1}$, from pp collisions at $\sqrt{s} = 8\,\text{TeV}$ collected by the LHCb experiment. The $\tau^+\tau^-$ candidates are reconstructed in final states with the first tau lepton decaying leptonically, and the second decaying either leptonically or to one or three charged hadrons. The production cross-section is measured for Z bosons with invariant mass between 60 and $120\,\text{GeV}/c^2$, which decay to tau leptons with transverse momenta greater than $20\,\text{GeV}/c$ and pseudorapidities between 2.0 and 4.5. The cross-section is determined to be $\sigma_{pp \to Z \to \tau^+\tau^-} = 95.8 \pm 2.1 \pm 4.6 \pm 0.2 \pm 1.1\,\text{pb}$, where the first uncertainty is statistical, the second is systematic, the third is due to the LHC beam energy uncertainty, and the fourth to the integrated luminosity uncertainty. This result is compatible with NNLO Standard model predictions. The ratio of the cross-sections for $Z \to \tau^+\tau^-$ to $Z \to \mu^+\mu^-$ ($Z \to e^+e^-$), determined to be 1.01 ± 0.05 (1.02 ± 0.06), is consistent with the lepton-universality hypothesis in Z decays.

https://doi.org/10.1007/JHEP09(2018)159

Contents

1 Introduction

The measurement of the production cross-section for a Z boson[1] using different decay modes in proton-proton (pp) collisions, $\sigma_{pp\to Z\to f\bar{f}}$, is an important verification of Standard Model (SM) predictions. The ratio of the $Z \to \tau^+\tau^-$ production cross-sections to other leptonic decay modes provides a test of lepton universality (LU). The LEP experiments have performed high accuracy tests of LU at the Z pole, with a precision better than 1% [1]. Consequently, the observation in proton-proton collisions of any apparent deviation from LU in Z decays would be an evidence of new phenomena producing final-state leptons, like in the theoretical context of mSUGRA [2], constrained NMSSM [3], Randall-Sundrum models [4, 5], or lepton-violating decays of Higgs-like bosons [6–10].

This analysis extends the LHCb results obtained with pp collisions at $\sqrt{s} = 7\,\text{TeV}$ [11] to $\sqrt{s} = 8\,\text{TeV}$. The cross-section is measured for leptons from the Z decay with transverse momentum (p_T) above $20\,\text{GeV}/c$ and a Z invariant mass between 60 and $120\,\text{GeV}/c^2$, as for the previously published $Z \to \mu^+\mu^-$ and $Z \to e^+e^-$ cross-sections [12, 13]. The cross-section measurements in the pseudorapidity range $2.0 < \eta < 4.5$ covered by the LHCb experiment are complementary to those with the central detectors ATLAS [14] and CMS [15].

In the present analysis, the reconstruction of the tau-pair candidates is performed in both leptonic and hadronic decay modes of the tau, requiring at least one leptonic mode for the tau-pair candidate. The reconstruction of high-p_T tau leptons in the 3-prong decay mode is performed for the first time in LHCb.

---

[1]Z refers to $Z/\gamma^\star$, i.e. includes contributions from the virtual photon production and interference.

2 Detector and datasets

The LHCb detector [16, 17] is a single-arm forward spectrometer designed for the study of particles containing b or c quarks. The detector includes a high-precision tracking system consisting of a silicon-strip vertex detector surrounding the pp interaction region, a large-area silicon-strip detector located upstream of a dipole magnet with a bending power of $4\,\mathrm{Tm}$, and three stations of silicon-strip detectors and straw drift tubes placed downstream of the magnet. The tracking system provides a measurement of momentum of charged particles with a relative uncertainty that varies from 0.5% at low momentum to 1.0% at $200\,\mathrm{GeV}/c$. The minimum distance of a track to a primary vertex (PV), the impact parameter (IP), is measured with a resolution of $(15 + 29/p_{\mathrm{T}})\,\mu\mathrm{m}$, where p_{T} is the component of the momentum transverse to the beam, in GeV/c. Photons, electrons and hadrons are identified by a calorimeter system consisting of scintillating-pad (SPD) and preshower detectors (PS), an electromagnetic calorimeter (ECAL) and a hadronic calorimeter (HCAL). Muons are identified by a system composed of five stations of alternating layers of iron and multiwire proportional chambers.

The online event selection is performed by a trigger, which consists of a hardware stage, based on information from the calorimeter and muon systems, followed by a software stage, which applies a full event reconstruction. The hardware trigger imposes a global event cut (GEC) requiring the hit multiplicity in the SPD to be less than 600, to prevent events with high occupancy from dominating the processing time in the software trigger.

This analysis uses pp collisions at $\sqrt{s} = 8\,\mathrm{TeV}$ corresponding to a total integrated luminosity of $\mathcal{L} = (1976 \pm 23)\,\mathrm{pb}^{-1}$ [18]. Simulated data samples are used to study the event selection, determine efficiencies, and estimate systematic uncertainties. In the simulation, pp collisions are generated using PYTHIA 8 [19, 20] with a specific LHCb configuration [21], and parton density functions taken from CTEQ6L [22]. Decays of hadronic particles are described by EvtGen [23], in which final-state radiation is generated using PHOTOS [24]. The interaction of the generated particles with the detector, and its response, are implemented using the GEANT4 toolkit [25, 26] as described in ref. [27].

3 Event selection

The Z boson is reconstructed from τ particles decaying into leptonic (muons or electrons) or hadronic (one or three charged hadrons) final states. Charged tracks are reconstructed by the tracking system and matched with clusters of ECAL/HCAL cells and hits in the muon detector. Muon candidates are identified by matching tracks to hits in the muon stations downstream of the calorimeters. They are required to leave hits in at least three muon stations, or four muon stations if they have $p_{\mathrm{T}} > 10\,\mathrm{GeV}/c$. Electron candidates must fail the muon identification criteria and fall within the acceptance of the PS, ECAL, and HCAL sub-detectors. On average, 30% of a material radiation length is crossed by a particle before the bending magnet, causing a considerable energy loss by bremsstrahlung for electrons and positrons. Hence, the electron or positron candidate momentum is corrected using a bremsstrahlung photon recovery technique [28]. However, since the ECAL

is designed to register particles from heavy-flavour hadron decays, calorimeter cells with transverse energy above about $10\,\text{GeV}$ saturate the electronics, and lead to incomplete electron bremsstrahlung recovery. A large energy deposit in the PS, ECAL, but not in HCAL is required, satisfying $E_{\text{PS}} > 50\,\text{MeV}$, $E_{\text{ECAL}}/p > 0.1$, and $E_{\text{HCAL}}/p < 0.05$, where p is the reconstructed momentum of the electron candidate, after applying the bremsstrahlung photon recovery. Charged hadrons are required to be within the HCAL acceptance, deposit an energy of $E_{\text{HCAL}}/p > 0.05$, and must fail the muon identification criteria. The pion mass is assigned to all charged hadrons.

The analysis is divided into seven "streams", labelled as $\tau_\mu\tau_\mu$, $\tau_\mu\tau_e$, $\tau_\mu\tau_{h1}$, $\tau_\mu\tau_{h3}$, $\tau_e\tau_e$, $\tau_e\tau_{h1}$, and $\tau_e\tau_{h3}$, where the subscript denotes the final state reconstructed. Charge-conjugate processes are implied throughout. The streams are chosen such that at least one τ lepton decays leptonically. The tau-pair candidates are selected by triggers requiring muons or electrons with a minimum transverse momentum of $15\,\text{GeV}/c$. The trigger efficiency is between 70% and 85%, depending on the number of leptons in the stream. The final states presented in this analysis account for 58% of all $Z \to \tau^+\tau^-$ decays. In the following, a τ candidate corresponds to a single particle for the τ_e, τ_μ, and τ_{h1} decay channels, or a combination of the three hadrons in the case of τ_{h3}. A pair of τ candidates must be associated to the same PV. In case where multiple PVs are presented in the event, the associated PV is defined as that with a smallest change in vertex-fit χ^2 when it is reconstructed with and without the τ candidate.

The dominating backgrounds are of QCD origin with one or several jets (call "QCD events" in the following), as well as electroweak processes, mainly W/Z +jets ("Vj"). The following requirements on the transverse momentum of τ decay products are used to reduce these backgrounds. For all the streams the triggering lepton must have $p_{\text{T}} > 20\,\text{GeV}/c$. For the processes $\tau_\mu\tau_\mu$, $\tau_e\tau_e$, and $\tau_\mu\tau_e$ the second lepton p_{T} threshold is $5\,\text{GeV}/c$. The hadron of the τ_{h1} candidates is required to have $p_{\text{T}} > 10\,\text{GeV}/c$. For the τ_{h3} decay channel, each of the three charged hadrons are selected with $p_{\text{T}} > 1\,\text{GeV}/c$, and at least one must be above $6\,\text{GeV}/c$. In addition, the τ_{h3} candidates must have a total p_{T} in excess of $12\,\text{GeV}/c$, and an invariant mass in the range 0.7 to $1.5\,\text{GeV}/c^2$. This leads to the τ_{h3} identification efficiency of about 30%, comparable with the value of 35% found in the context of the $B^0 \to D^{*-}\tau^+\nu_\tau$ analysis [29]. For all streams, the reconstructed direction of the τ candidate must be in the fiducial geometrical acceptance $2.0 < \eta < 4.5$.

Additional selection criteria are needed to suppress background processes due to semileptonic c- or b-hadron decays, misidentification of hadrons as leptons, or, especially in the τ_{h3} stream, combinations of unrelated particles.

Signal candidates tend to have back-to-back tracks in the plane transverse to the beam axis, and a higher invariant mass than the background. Hence, the tau-pair is required to have an invariant mass above $20\,\text{GeV}/c^2$, or $30\,\text{GeV}/c^2$ for the stream containing τ_{h1}, τ_{h3} candidates. Additionally, for the dilepton streams $\tau_\mu\tau_\mu$, $\tau_e\tau_e$, the selected mass range is below $60\,\text{GeV}/c^2$, to avoid the on-shell $Z \to \mu^+\mu^-$ and $Z \to e^+e^-$ regions. The absolute difference in azimuthal angle of the two τ candidates is required to be greater than 2.7 radians. The above selections are found to be 70 to 80% efficient, depending on the analysis stream.

Charged particles in QCD events tend to be associated with jet activity, in contrast to signal candidates where they are isolated. An isolation variable, $\hat{I}_{p_\mathrm{T}}$, is defined as the p_T of the candidate divided by the transverse component of the vectorial sum of all track momenta in a cone surrounding the candidate of radius $R_{\eta\phi} = 0.5$, defined in the pseudorapidity-azimuthal angle $(\eta-\phi)$ space. A fully isolated candidate has $\hat{I}_{p_\mathrm{T}} = 1$, while lower values indicate the presence of jet activity. The selection $\hat{I}_{p_\mathrm{T}} > 0.9$ is applied to all τ candidates, with an efficiency of more than 64% for the tau-pair signal and rejecting about 98% of QCD events.

The lifetime of the τ lepton is used to separate the signal from prompt background. For the τ decay channels with a single charged particle, it is not possible to reconstruct a secondary vertex and a selection on the particle IP to the associated PV is applied. The efficiency on the signal from these criteria is in the range 71 to 79%.

In the τ_{h3} case, a vertex reconstruction is possible: the maximum distance between the three tracks in the $\eta - \phi$ space is required to be less than $0.005 \cdot p_\mathrm{T}$ where p_T is the transverse momentum of τ_{h3} in GeV/c. The proper decay time is subsequently estimated from the distance of the reconstructed vertex to the associated PV, and the momentum of the candidate, taken as an approximation of the τ momentum. A minimum of 60 fs is imposed for this variable, efficiently discarding the prompt background whilst keeping about 77% of the signal. For the τ_{h3} decay, a correction to the mass is also possible by exploiting the direction of flight, recovering part of the momentum lost due to undetected particles. The corrected mass is defined as

$$m_{\mathrm{corr}} \equiv \sqrt{m^2 + p^2 \sin^2\theta} + p\sin\theta\,, \tag{3.1}$$

where m and p are the invariant mass and momentum computed from the three tracks and θ is the angle between the momentum and flight direction of the candidate. The requirement $m_{\mathrm{corr}} < 3\,\mathrm{GeV}/c^2$ reduces the QCD background by about 50% and the Vj background by about 60%, retaining 80% of the signal. Figure 1 shows the mass distributions of τ_{h3} candidates before and after correction for data, compared to the distributions of $Z \to \tau^+\tau^-$ decays and of the Vj background from simulation.

In the $\tau_e\tau_e$ and $\tau_\mu\tau_\mu$ streams an additional background component arises from $Z \to l^+l^-$ decays. This process produces two muons or two electrons with similar p_T values, in contrast to signal which tends to have unbalanced p_T due to the missing momentum from unreconstructed neutrinos and neutral hadrons. The p_T asymmetry, A_{p_T}, is defined as the absolute p_T difference of the two candidates divided by their sum. For the two leptonic streams A_{p_T} is required to be greater than 0.1. A particular case is the $\tau_\mu\tau_e$ stream, where background from Vj processes arises, with one lepton coming from the jet causing a relatively large p_T imbalance with respect to the lepton from the W/Z boson. A suppression by a factor of two of this source of background, with a loss of 10% of the signal is obtained imposing a maximal A_{p_T} value of 0.6. For τ_{h1} and τ_{h3} the A_{p_T} criterion has been found inefficient for background rejection, hence no such a constraint is imposed to these two decay modes.
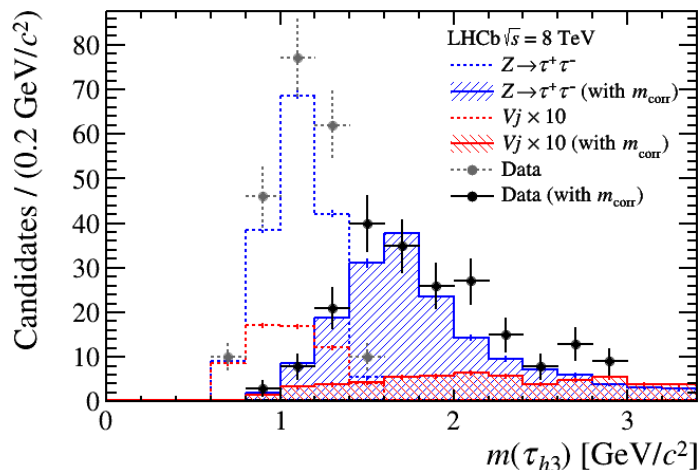
Figure 1. Distributions of invariant (dashed line) and corrected (full line, shaded) mass of τ_{h3} candidates from the $\tau_\mu\tau_{h3}$ channel. The yields are normalised to the integrated luminosity of the data. The results from data are represented by the black points. The error bars represent the statistical uncertainty only. The distributions are compared to the signal distributions from simulated $Z\to\tau^+\tau^-$ (blue) events and the Vj (red) background.

	$\tau_\mu\tau_\mu$	$\tau_\mu\tau_{h1}$	$\tau_\mu\tau_{h3}$	$\tau_e\tau_e$	$\tau_e\tau_{h1}$	$\tau_e\tau_{h3}$	$\tau_\mu\tau_e$
$Z\to l^+l^-$	249.7(88)	1.2(5)	—	420.8(253)	16.1(22)	—	25.3(54)
QCD	50.9(102)	235.8(193)	21.2(53)	42.7(88)	330.8(228)	19.4(51)	160.0(169)
Vj	12.7(74)	144.2(430)	5.1(34)	5.8(27)	68.3(197)	10.1(58)	65.3(257)
VV	0.2(1)	1.2(2)	0.2(1)	0.2(1)	0.8(1)	0.2(1)	10.0(5)
$t\bar t$	1.0(2)	2.2(2)	0.6(1)	0.2()	0.7(1)	0.1()	5.5(2)
$Z\to b\bar b$	0.8(4)	0.3(2)	0.1(1)	0.1(1)	0.3(2)	0.1(1)	0.3(2)
Cross-feed	4.5(11)	22.2(25)	13.9(20)	13.0(39)	16.5(24)	7.3(17)	52.5(42)
Total bkg.	319.9(127)	407.1(375)	41.1(53)	482.7(242)	433.5(220)	37.2(58)	318.9(236)
Observed	696	1373	205	610	861	110	1322
$Z\to\tau^+\tau^-$	376.1(290)	965.9(521)	163.9(142)	127.3(329)	427.5(358)	72.8(111)	1003.1(418)

Table 1. Expected backgrounds yields and total number of candidates observed. In the last row the uncertainties are the statistical and systematic contributions combined.

4 Signal and background estimation

After the selections described in the previous section, a maximum of one $Z\to\tau^+\tau^-$ candidate per event is found. The number of signal candidates is determined from the number of observed candidates in data subtracted by the total number of estimated backgrounds. The results are summarized in table 1. The invariant-mass distributions for such candidates are shown in figure 2, for the seven analysis streams.

A data-driven approach is used to estimate the amount of background from QCD and Vj processes. Same-sign (SS) tau-pair candidates are selected with identical criteria as the signal, but requiring the tau candidates to have identical electric charge. From simulation, the SS candidates yield is found to originate mainly from QCD and Vj processes, while
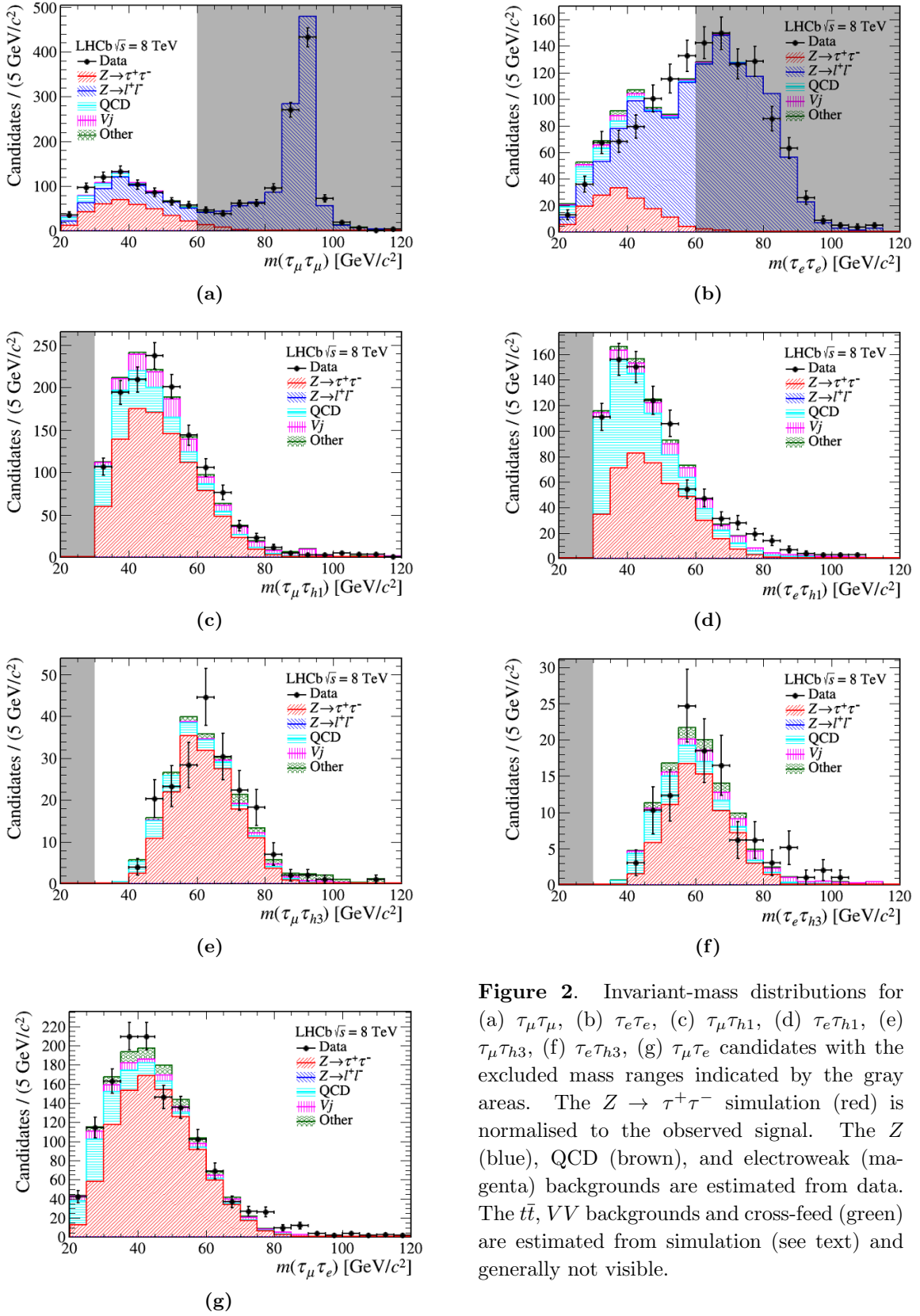
Figure 2. Invariant-mass distributions for (a) $\tau_\mu\tau_\mu$, (b) $\tau_e\tau_e$, (c) $\tau_\mu\tau_{h1}$, (d) $\tau_e\tau_{h1}$, (e) $\tau_\mu\tau_{h3}$, (f) $\tau_e\tau_{h3}$, (g) $\tau_\mu\tau_e$ candidates with the excluded mass ranges indicated by the gray areas. The $Z \to \tau^+\tau^-$ simulation (red) is normalised to the observed signal. The Z (blue), QCD (brown), and electroweak (magenta) backgrounds are estimated from data. The $t\bar{t}$, VV backgrounds and cross-feed (green) are estimated from simulation (see text) and generally not visible.

the mis-reconstructed $Z \to \tau^+\tau^-$ process contributes less than 1%: $N^{\mathrm{SS}} = N^{\mathrm{SS}}_{\mathrm{QCD}} + N^{\mathrm{SS}}_{Vj} + N^{\mathrm{SS}}_{Z \to \tau^+\tau^-}$. The last term originates, for instance, from an electron either from a π^0 decay or pair-production, a single hadron from partially-reconstructed τ_{h3}, 3-prong from false combinatorics, or a muon from a misidentified hadron. The amount of QCD and Vj events in the SS dataset is determined by a fit to the $p_{\mathrm{T}}(\tau_1) - p_{\mathrm{T}}(\tau_2)$ distribution, for each analysis stream [11]. In the fit, the QCD distribution templates are taken from an SS QCD-enriched dataset, obtained by the anti-isolation requirement $\hat{I}_{p_{\mathrm{T}}} < 0.6$; the distributions templates for the two Vj processes (W+jet, Z+jet) are obtained from simulation and are found to be statistically consistent. Subsequently, the number of QCD and Vj background candidates is computed as $N_{\mathrm{QCD}} = r_{\mathrm{QCD}} \cdot N^{\mathrm{SS}}_{\mathrm{QCD}}$, and $N_{Vj} = r_{Vj} \cdot N^{\mathrm{SS}}_{Vj}$. The value of r_{Vj} is obtained from simulation, considering both W and Z contributions, and varies from 1.05 ± 0.08 for the $\tau_e\tau_e$ up to 2.37 ± 0.30 for the $\tau_\mu\tau_{h1}$. The same-sign and opposite-sign QCD-enriched datasets provide the r_{QCD} values, which are all close to unity, with the exception of 1.30 ± 0.05, obtained for $\tau_\mu\tau_\mu$.

The $Z \to l^+l^-$ decays ($l = e, \mu$) are a background for all the streams, except for $\tau_\mu\tau_{h3}$ and $\tau_e\tau_{h3}$. The number of $Z \to l^+l^-$ decays contaminating the $\tau_\mu\tau_\mu$ stream is determined by applying all selection criteria except for the requirement on the dimuon mass: this produces a sample with a clear peak at the Z mass, as well as an off-shell contribution at lower mass, as shown in figure 2a. A template distribution obtained from simulation is normalised to the data in the 80–100 GeV/c^2 mass interval. The fraction of genuine $Z \to \tau^+\tau^-$ candidates in the normalisation region is found to be negligible from simulation. The contribution from $Z \to \mu^+\mu^-$ decays to the background in the signal region is inferred from the normalised distribution. A similar procedure is applied to estimate the $\tau_e\tau_e$ background from $Z \to e^+e^-$ decays, but with the normalisation performed in the 70–100 GeV/c^2 interval to account for the electron momentum resolution degraded by an incomplete electron bremsstrahlung recovery. For this process, 1% of non-Z background candidates are subtracted from the normalisation region, as estimated from SS dilepton events.

The process $Z \to \mu^+\mu^-$ can be observed as a fake $\tau_\mu\tau_{h1}$ candidate when one of the muons is misidentified as a charged hadron. This background is evaluated by applying the $\tau_\mu\tau_{h1}$ selection but requiring a second identified muon rather than a hadron, and scaling by the probability for a muon to be misidentified as a hadron. The misidentification probability, obtained from simulation and cross-checked using a tag-and-probe method applied to $Z \to \mu^+\mu^-$ data (requiring an identified muon as a tag, and an oppositely-charged track as a probe), is of the order of 10^{-3} for muons with $p_{\mathrm{T}} < 10\,\mathrm{GeV}/c$, and 10^{-4}–10^{-5} at larger p_{T} values. The uncertainty on the estimation of this background is obtained from the lepton misidentification probability uncertainty combined with the statistical uncertainty of the dimuon candidates sample. A similar procedure allows the estimation of $Z \to \mu^+\mu^-$, $Z \to e^+e^-$ backgrounds in $\tau_\mu\tau_e$, $\tau_e\tau_{h1}$ streams.

Other background processes are due to diboson decays, $t\bar{t}$ events, and Z decays into b hadrons. Their contributions are relatively small and obtained from simulation.

Some of the selected tau-pair candidates may not originate from the stream under study. For instance, a τ_{h1} candidate may be selected from a partially reconstructed τ_{h3} candidate. The fraction of cross-feed candidates is obtained from the $Z \to \tau^+\tau^-$ simulated

sample. The statistical uncertainty is 1 to 3%, to which a small contribution from the uncertainties on the branching fractions of the contaminating streams is added.

5 Cross-section measurement

The production cross-section of Z boson to tau-pair is measured for each analysis stream using

$$\sigma_{pp \to Z \to \tau^+ \tau^-} = \frac{N_{\text{obs}}/\varepsilon_{\text{rec}}^{\text{obs}} - \sum_k N_{\text{bkg,k}}/\varepsilon_{\text{rec}}^{\text{bkg,k}}}{\mathcal{L} \, \mathcal{B} \, \mathcal{A} \, \varepsilon_{\text{sel}}}, \tag{5.1}$$

where N_{obs} is the number of observed Z bosons and $N_{\text{bkg,k}}$ is the estimated background from source k.

The total integrated luminosity is denoted by $\mathcal{L}$, and $\mathcal{B}$ is the product of the branching fractions of the tau lepton pair to decay to the given final state, with values and uncertainties taken from the world averages [30]. The acceptance factor, $\mathcal{A}$, is needed to normalise the results of each analysis stream to the kinematical region $60 < M_{\tau\tau} < 120$ GeV/c^2, $2.0 < \eta^\tau < 4.5$, and $p_{\text{T}}^\tau > 20$ GeV/c, which allows the comparison with the $Z \to \mu^+\mu^-$, $Z \to e^+e^-$ decay measurements in LHCb [12, 13]. This factor is the fraction of $Z \to \tau^+\tau^-$ events where the generated τ satisfy the chosen kinematical selections, which also fulfill the fiducial acceptance selection. The value of $\mathcal{A}$ for each stream is obtained from simulation, using the POWHEG-BOX [31–34] at next-to-leading order with PDF MSTW08NLO90cl [35], and PYTHIA 8.175 [19, 20]. The uncertainty on $\mathcal{A}$ from the choice of PDF is estimated following the procedure explained in ref. [36].

The event reconstruction and selection efficiencies, ε_{rec} and ε_{sel}, as well as their uncertainties, are estimated from simulation and calibrated using a data-driven method (where applicable) derived from the method described in refs. [11–13]. The term ε_{rec} is the product of the GEC, trigger, tracking and particle identification efficiencies. The smallest value of ε_{rec} is found to be 9% in the $\tau_e\tau_{h3}$ stream, while the largest value is 65% for $\tau_\mu\tau_\mu$. The GEC efficiency is determined from $Z \to l^+l^-$ decays in data collected with a relaxed requirement. The muon and electron trigger efficiencies are evaluated as a function of η and p_{T} using a tag-and-probe method applied on $Z \to l^+l^-$ decays. The tracking efficiency for muons uses a tag-and-probe method from $Z \to \mu^+\mu^-$ decays in data, whereas for electrons and charged hadrons simulated samples are used. The particle identification efficiency is also obtained by a tag-and-probe procedure. In order to cover the signal p_{T} spectrum, different data samples are selected: $Z \to \mu^+\mu^-$ and $J/\psi \to \mu^+\mu^-$ decays for muons, $Z \to e^+e^-$ and $B^+ \to J/\psi(\to e^+e^-)K^+$ decays for electrons, and $D^{*+} \to D^0(\to K^-\pi^+)\pi^+$ decays for charged hadrons.

The efficiency of the selection ranges between 20% for $\tau_e\tau_e$ and 50% for $\tau_\mu\tau_e$. The values are obtained from the simulation. Corrections at the level of 1% are inferred by the comparison of the selection-variable distributions for $Z \to \mu^+\mu^-$ decays in data and simulated samples, which are also added to the systematic uncertainty.

A summary of uncertainties is given in table 2, with the statistical uncertainty from N_{obs} obtained assuming Poissonian statistics. The contribution of the LHC beam energy uncertainty [37] is of 0.2% as studied with the DYNNLO generator [38]. The integrated

	$\tau_\mu\tau_\mu$	$\tau_\mu\tau_{h1}$	$\tau_\mu\tau_{h3}$	$\tau_e\tau_e$	$\tau_e\tau_{h1}$	$\tau_e\tau_{h3}$	$\tau_\mu\tau_e$
Tau branching fractions product	0.5	0.3	0.5	0.5	0.3	0.5	0.3
PDF, acceptance, FSR	1.3	1.9	1.5	1.3	1.9	1.5	1.3
Reconstruction	2.1	3.1	5.6	4.5	5.4	7.0	2.7
Selection	5.0	3.5	4.7	5.7	3.5	5.1	3.9
Background estimation†	3.4	3.9	3.2	19.0	5.2	8.0	2.4
Systematic	6.4	6.2	8.0	20.3	8.4	11.8	5.2
Statistical†	6.9	3.8	8.1	17.6	6.6	13.1	3.4
Beam energy	0.2	0.2	0.2	0.2	0.2	0.2	0.2
Luminosity	1.2	1.2	1.2	1.2	1.2	1.2	1.2
Total	9.6	7.5	11.5	27.0	10.8	17.7	6.5

Table 2. Relative uncertainties of the various contributions affecting the cross-section measurement, given in percent. The uncertainties are correlated between streams, except in rows denoted with †.

luminosity is measured using van der Meer scans [39] and beam-gas imaging method [40], giving a combined uncertainty of 1.2% [18].

The cross-section results compared with the previous $Z \to \mu^+\mu^-$ and $Z \to e^+e^-$ measurements inside the same acceptance region at 8 TeV [12, 13], are presented in figure 3, where the region is defined for Z bosons with an invariant mass between 60 and 120 GeV/c^2 decaying to leptons with $p_T > 20$ GeV/c and $2.0 < \eta < 4.5$. The predictions from theoretical models are calculated with the FEWZ [41, 42] generator at NNLO for the PDF sets ABM12 [43], CT10 [44], CT14 [45], HERA15 [46], MSTW08 [35], MMHT14 [47], and NNPDF30 [48]. A best linear unbiased estimator is used to combine the measurements from all streams taking into account their correlations, giving a χ^2 per degree of freedom of 0.69 (p-value of 0.658). The combined cross-section is

$$\sigma_{pp \to Z \to \tau^+\tau^-} = 95.8 \pm 2.1 \pm 4.6 \pm 0.2 \pm 1.1 \, \text{pb} \,,$$

where the uncertainties are statistical, systematic, due to the LHC beam energy uncertainty, and to the integrated luminosity uncertainty, respectively.

Lepton universality is tested from the cross-section ratios [12, 13]

$$\frac{\sigma^{8\,\text{TeV}}_{pp \to Z \to \tau^+\tau^-}}{\sigma^{8\,\text{TeV}}_{pp \to Z \to \mu^+\mu^-}} = 1.01 \pm 0.05 \,, \qquad \frac{\sigma^{8\,\text{TeV}}_{pp \to Z \to \tau^+\tau^-}}{\sigma^{8\,\text{TeV}}_{pp \to Z \to e^+e^-}} = 1.02 \pm 0.06 \,,$$

where the uncertainties due to the LHC beam energy and to the integrated luminosity are assumed to be fully correlated as the analyses share the same dataset, whilst the statistical and systematic uncertainties are assumed to be uncorrelated.

6 Conclusion

A measurement of $Z \to \tau^+\tau^-$ production cross-section in pp collisions at $\sqrt{s} = 8$ TeV inside LHCb fiducial acceptance region is reported, where the region is defined as a tau-
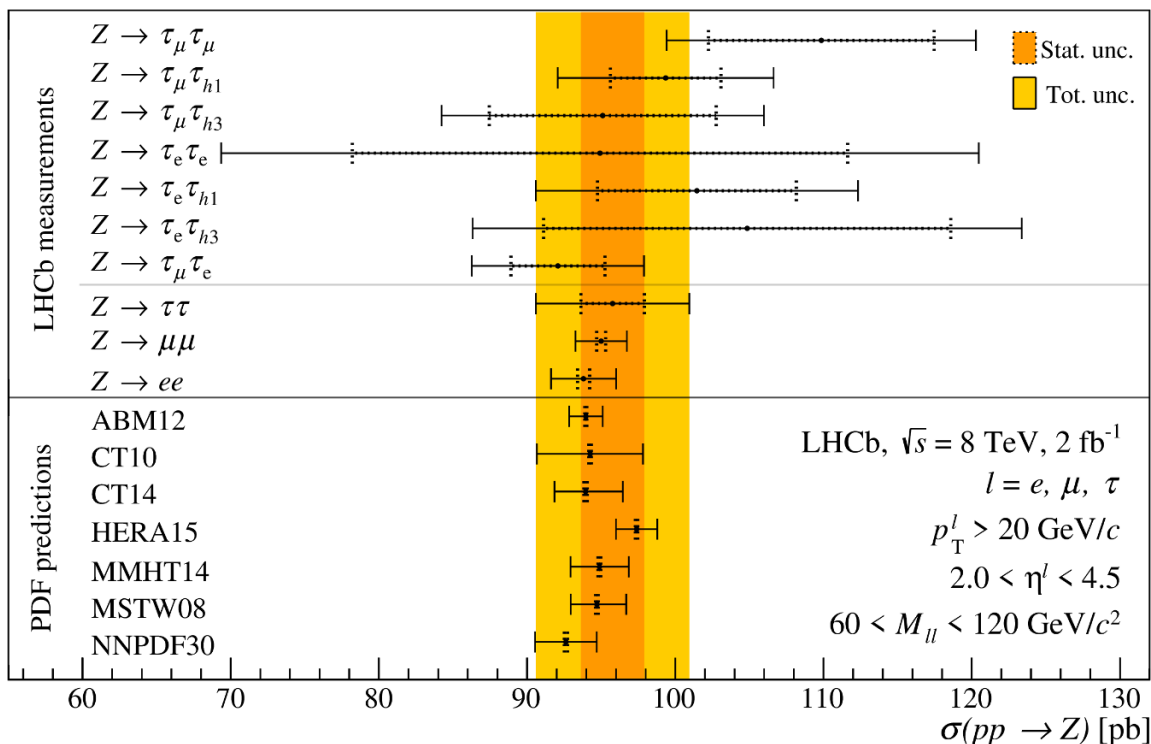
Figure 3. Summary of the measurements of $Z \to l^+l^-$ production cross-section inside the LHCb acceptance region from pp collisions at 8 TeV. The error bar represents the total uncertainty. The dotted inner error bar corresponds to the statistical contribution. The coloured band corresponds to the combined measurement of $Z \to \tau^+\tau^-$ from this analysis. The last 7 rows represent the NNLO predictions with different parameterizations of the PDFs.

pair of invariant mass between 60 and 120 GeV/c^2, with the tau leptons having a transverse momentum greater than 20 GeV/c, and pseudorapidity between 2.0 and 4.5.

The reconstruction of tau-pair candidates is performed in both leptonic and hadronic decay modes of the tau lepton, requiring at least one leptonic mode for the tau-pair combination. The backgrounds to $Z \to \tau^+\tau^-$ are mainly from QCD and W/Z +jets and are estimated with a data-driven method.

The production cross-section with all uncertainties summed in quadrature yields 95.8(52) pb, in agreement with the SM prediction. The results are consistent with the $Z \to e^+e^-$ and $Z \to \mu^+\mu^-$ cross-sections measured at LHCb. They are compatible with LU at the level of 6%.

Acknowledgments

References

[1] SLD Electroweak Group, Heavy Flavour Group, LEP Electroweak Working Group, OPAL, DELPHI, ALEPH, SLD and L3 collaborations, S. Schael et al., *Precision electroweak measurements on the Z resonance*, *Phys. Rept.* **427** (2006) 257 [hep-ex/0509008] [inSPIRE].

[2] F. Heinemann, *The Discovery potential of the $\tilde{\chi}_2^0$ in mSUGRA in the τ-channel at high $\tan\beta$ at the LHC*, Ph.D. Thesis, ETH, Zurich Switzerland (2003), [hep-ex/0406056] [inSPIRE].

[3] U. Ellwanger, A. Florent and D. Zerwas, *Discovering the constrained NMSSM with tau leptons at the LHC*, *JHEP* **01** (2011) 103 [arXiv:1011.0931] [inSPIRE].

[4] G. Perez and L. Randall, *Natural Neutrino Masses and Mixings from Warped Geometry*, *JHEP* **01** (2009) 077 [arXiv:0805.4652] [inSPIRE].

[5] S. Casagrande, F. Goertz, U. Haisch, M. Neubert and T. Pfoh, *Flavor Physics in the Randall-Sundrum Model: I. Theoretical Setup and Electroweak Precision Tests*, *JHEP* **10** (2008) 094 [arXiv:0807.4937] [inSPIRE].

[6] R. Harnik, J. Kopp and J. Zupan, *Flavor Violating Higgs Decays*, *JHEP* **03** (2013) 026 [arXiv:1209.1397] [inSPIRE].

[7] G. Blankenburg, J. Ellis and G. Isidori, *Flavour-Changing Decays of a 125 GeV Higgs-like Particle*, *Phys. Lett.* **B 712** (2012) 386 [arXiv:1202.5704] [inSPIRE].

[8] J.L. Diaz-Cruz and J.J. Toscano, *Lepton flavor violating decays of Higgs bosons beyond the standard model*, *Phys. Rev.* **D 62** (2000) 116005 [hep-ph/9910233] [inSPIRE].

[9] A. Goudelis, O. Lebedev and J.-h. Park, *Higgs-induced lepton flavor violation*, *Phys. Lett.* **B 707** (2012) 369 [arXiv:1111.1715] [inSPIRE].

[10] A. Arhrib, Y. Cheng and O.C.W. Kong, *Comprehensive analysis on lepton flavor violating Higgs boson to $\mu^{\mp}\tau^{\pm}$ decay in supersymmetry without R parity*, *Phys. Rev.* **D 87** (2013) 015025 [arXiv:1210.8241] [INSPIRE].

[11] LHCb collaboration, *A study of the Z production cross-section in pp collisions at $\sqrt{s} = 7\,TeV$ using tau final states*, *JHEP* **01** (2013) 111 [arXiv:1210.6289] [INSPIRE].

[12] LHCb collaboration, *Measurement of forward W and Z boson production in pp collisions at $\sqrt{s} = 8\,TeV$*, *JHEP* **01** (2016) 155 [arXiv:1511.08039] [INSPIRE].

[13] LHCb collaboration, *Measurement of forward $Z \to e^+e^-$ production at $\sqrt{s} = 8\,TeV$*, *JHEP* **05** (2015) 109 [arXiv:1503.00963] [INSPIRE].

[14] ATLAS collaboration, *Simultaneous measurements of the $t\bar{t}$, W^+W^- and $Z/\gamma^* \to \tau\tau$ production cross-sections in pp collisions at $\sqrt{s} = 7\,TeV$ with the ATLAS detector*, *Nucl. Part. Phys. Proc.* **273–275** (2016) 2192 [INSPIRE].

[15] CMS collaboration, *Measurement of the inclusive Z cross section via decays to tau pairs in pp collisions at $\sqrt{s} = 7\,TeV$*, *JHEP* **08** (2011) 117 [arXiv:1104.1617] [INSPIRE].

[16] LHCb collaboration, *The LHCb Detector at the LHC*, 2008 *JINST* **3** S08005 [INSPIRE].

[17] LHCb collaboration, *LHCb Detector Performance*, *Int. J. Mod. Phys.* **A 30** (2015) 1530022 [arXiv:1412.6352] [INSPIRE].

[18] LHCb collaboration, *Precision luminosity measurements at LHCb*, 2014 *JINST* **9** P12005 [arXiv:1410.0149] [INSPIRE].

[19] T. Sjöstrand, S. Mrenna and P.Z. Skands, *A Brief Introduction to PYTHIA 8.1*, *Comput. Phys. Commun.* **178** (2008) 852 [arXiv:0710.3820] [INSPIRE].

[20] T. Sjöstrand, S. Mrenna and P.Z. Skands, *PYTHIA 6.4 Physics and Manual*, *JHEP* **05** (2006) 026 [hep-ph/0603175] [INSPIRE].

[21] LHCb collaboration, *Handling of the generation of primary events in Gauss, the LHCb simulation framework*, *J. Phys. Conf. Ser.* **331** (2011) 032047 [INSPIRE].

[22] J. Pumplin, D.R. Stump, J. Huston, H.L. Lai, P.M. Nadolsky and W.K. Tung, *New generation of parton distributions with uncertainties from global QCD analysis*, *JHEP* **07** (2002) 012 [hep-ph/0201195] [INSPIRE].

[23] D.J. Lange, *The EvtGen particle decay simulation package*, *Nucl. Instrum. Meth.* **A 462** (2001) 152 [INSPIRE].

[24] P. Golonka and Z. Was, *PHOTOS Monte Carlo: A Precision tool for QED corrections in Z and W decays*, *Eur. Phys. J.* **C 45** (2006) 97 [hep-ph/0506026] [INSPIRE].

[25] GEANT4 collaboration, J. Allison et al., *Geant4 developments and applications*, *IEEE Trans. Nucl. Sci.* **53** (2006) 270 [INSPIRE].

[26] GEANT4 collaboration, S. Agostinelli et al., *GEANT4: A Simulation toolkit*, *Nucl. Instrum. Meth.* **A 506** (2003) 250 [INSPIRE].

[27] LHCb collaboration, *The LHCb simulation application, Gauss: Design, evolution and experience*, *J. Phys. Conf. Ser.* **331** (2011) 032023 [INSPIRE].

[28] LHCb collaboration, *LHCb calorimeters and muon system lepton identification*, *AIP Conf. Proc.* **722** (2004) 123.

[29] LHCb collaboration, *Measurement of the ratio of the $B^0 \to D^{*-}\tau^+\nu_\tau$ and $B^0 \to D^{*-}\mu^+\nu_\mu$ branching fractions using three-prong τ-lepton decays*, *Phys. Rev. Lett.* **120** (2018) 171802 [arXiv:1708.08856] [INSPIRE].

[30] Particle Data Group collaboration, C. Patrignani et al., *Review of Particle Physics*, *Chin. Phys.* **C 40** (2016) 100001 [inSPIRE].

[31] S. Alioli, P. Nason, C. Oleari and E. Re, *NLO vector-boson production matched with shower in POWHEG*, *JHEP* **07** (2008) 060 [arXiv:0805.4802] [inSPIRE].

[32] P. Nason, *A New method for combining NLO QCD with shower Monte Carlo algorithms*, *JHEP* **11** (2004) 040 [hep-ph/0409146] [inSPIRE].

[33] S. Frixione, P. Nason and C. Oleari, *Matching NLO QCD computations with Parton Shower simulations: the POWHEG method*, *JHEP* **11** (2007) 070 [arXiv:0709.2092] [inSPIRE].

[34] S. Alioli, P. Nason, C. Oleari and E. Re, *A general framework for implementing NLO calculations in shower Monte Carlo programs: the POWHEG BOX*, *JHEP* **06** (2010) 043 [arXiv:1002.2581] [inSPIRE].

[35] A.D. Martin, W.J. Stirling, R.S. Thorne and G. Watt, *Parton distributions for the LHC*, *Eur. Phys. J.* **C 63** (2009) 189 [arXiv:0901.0002] [inSPIRE].

[36] M. Botje et al., *The PDF4LHC Working Group Interim Recommendations*, arXiv:1101.0538 [inSPIRE].

[37] E. Todesco and J. Wenninger, *Large Hadron Collider momentum calibration and accuracy*, *Phys. Rev. Accel. Beams* **20** (2017) 081003 [inSPIRE].

[38] S. Catani, L. Cieri, G. Ferrera, D. de Florian and M. Grazzini, *Vector boson production at hadron colliders: a fully exclusive QCD calculation at NNLO*, *Phys. Rev. Lett.* **103** (2009) 082001 [arXiv:0903.2120] [inSPIRE].

[39] S. van der Meer, *Calibration of the effective beam height in the ISR*, CERN-ISR-PO-68-31 (1968) [inSPIRE].

[40] M. Ferro-Luzzi, *Proposal for an absolute luminosity determination in colliding beam experiments using vertex detection of beam-gas interactions*, *Nucl. Instrum. Meth.* **A 553** (2005) 388 [inSPIRE].

[41] Y. Li and F. Petriello, *Combining QCD and electroweak corrections to dilepton production in FEWZ*, *Phys. Rev.* **D 86** (2012) 094034 [arXiv:1208.5967] [inSPIRE].

[42] R. Gavin, Y. Li, F. Petriello and S. Quackenbush, *FEWZ 2.0: A code for hadronic Z production at next-to-next-to-leading order*, *Comput. Phys. Commun.* **182** (2011) 2388 [arXiv:1011.3540] [inSPIRE].

[43] S. Alekhin, J. Blumlein and S. Moch, *The ABM parton distributions tuned to LHC data*, *Phys. Rev.* **D 89** (2014) 054028 [arXiv:1310.3059] [inSPIRE].

[44] H.-L. Lai et al., *New parton distributions for collider physics*, *Phys. Rev.* **D 82** (2010) 074024 [arXiv:1007.2241] [inSPIRE].

[45] S. Dulat et al., *New parton distribution functions from a global analysis of quantum chromodynamics*, *Phys. Rev.* **D 93** (2016) 033006 [arXiv:1506.07443] [inSPIRE].

[46] ZEUS and H1 collaborations, F.D. Aaron et al., *Combined Measurement and QCD Analysis of the Inclusive $e^{\pm}p$ Scattering Cross Sections at HERA*, *JHEP* **01** (2010) 109 [arXiv:0911.0884] [inSPIRE].

[47] L.A. Harland-Lang, A.D. Martin, P. Motylinski and R.S. Thorne, *Parton distributions in the LHC era: MMHT 2014 PDFs*, *Eur. Phys. J.* **C 75** (2015) 204 [arXiv:1412.3989] [inSPIRE].

[48] NNPDF collaboration, R.D. Ball et al., *Parton distributions for the LHC Run II*, *JHEP* **04** (2015) 040 [arXiv:1410.8849] [inSPIRE].

The LHCb collaboration

R. Aaij[27], B. Adeva[41], M. Adinolfi[48], C.A. Aidala[73], Z. Ajaltouni[5], S. Akar[59], P. Albicocco[18],
J. Albrecht[10], F. Alessio[42], M. Alexander[53], A. Alfonso Albero[40], S. Ali[27], G. Alkhazov[33],
P. Alvarez Cartelle[55], A.A. Alves Jr[59], S. Amato[2], S. Amerio[23], Y. Amhis[7], L. An[3],
L. Anderlini[17], G. Andreassi[43], M. Andreotti[16,g], J.E. Andrews[60], R.B. Appleby[56], F. Archilli[27],
P. d'Argent[12], J. Arnau Romeu[6], A. Artamonov[39], M. Artuso[61], K. Arzymatov[37], E. Aslanides[6],
M. Atzeni[44], S. Bachmann[12], J.J. Back[50], S. Baker[55], V. Balagura[7,b], W. Baldini[16], A. Baranov[37],
R.J. Barlow[56], S. Barsuk[7], W. Barter[56], F. Baryshnikov[70], V. Batozskaya[31], B. Batsukh[61],
V. Battista[43], A. Bay[43], J. Beddow[53], F. Bedeschi[24], I. Bediaga[1], A. Beiter[61], L.J. Bel[27],
N. Beliy[63], V. Bellee[43], N. Belloli[20,i], K. Belous[39], I. Belyaev[34,42], E. Ben-Haim[8], G. Bencivenni[18],
S. Benson[27], S. Beranek[9], A. Berezhnoy[35], R. Bernet[44], D. Berninghoff[12], E. Bertholet[8],
A. Bertolin[23], C. Betancourt[44], F. Betti[15,42], M.O. Bettler[49], M. van Beuzekom[27],
Ia. Bezshyiko[44], S. Bhasin[48], J. Bhom[29], S. Bifani[47], P. Billoir[8], A. Birnkraut[10], A. Bizzeti[17,u],
M. Bjørn[57], M.P. Blago[42], T. Blake[50], F. Blanc[43], S. Blusk[61], D. Bobulska[53], V. Bocci[26],
O. Boente Garcia[41], T. Boettcher[58], A. Bondar[38,w], N. Bondar[33], S. Borghi[56,42], M. Borisyak[37],
M. Borsato[41,42], F. Bossu[7], M. Boubdir[9], T.J.V. Bowcock[54], C. Bozzi[16,42], S. Braun[12],
M. Brodski[42], J. Brodzicka[29], D. Brundu[22], E. Buchanan[48], A. Buonaura[44], C. Burr[56],
A. Bursche[22], J. Buytaert[42], W. Byczynski[42], S. Cadeddu[22], H. Cai[64], R. Calabrese[16,g],
R. Calladine[47], M. Calvi[20,i], M. Calvo Gomez[40,m], A. Camboni[40,m], P. Campana[18],
D.H. Campora Perez[42], L. Capriotti[56], A. Carbone[15,e], G. Carboni[25], R. Cardinale[19,h],
A. Cardini[22], P. Carniti[20,i], L. Carson[52], K. Carvalho Akiba[2], G. Casse[54], L. Cassina[20],
M. Cattaneo[42], G. Cavallero[19,h], R. Cenci[24,p], D. Chamont[7], M.G. Chapman[48], M. Charles[8],
Ph. Charpentier[42], G. Chatzikonstantinidis[47], M. Chefdeville[4], V. Chekalina[37], C. Chen[3],
S. Chen[22], S.-G. Chitic[42], V. Chobanova[41], M. Chrzaszcz[42], A. Chubykin[33], P. Ciambrone[18],
X. Cid Vidal[41], G. Ciezarek[42], P.E.L. Clarke[52], M. Clemencic[42], H.V. Cliff[49], J. Closier[42],
V. Coco[42], J. Cogan[6], E. Cogneras[5], L. Cojocariu[32], P. Collins[42], T. Colombo[42],
A. Comerma-Montells[12], A. Contu[22], G. Coombs[42], S. Coquereau[40], G. Corti[42], M. Corvo[16,g],
C.M. Costa Sobral[50], B. Couturier[42], G.A. Cowan[52], D.C. Craik[58], A. Crocombe[50],
M. Cruz Torres[1], R. Currie[52], C. D'Ambrosio[42], F. Da Cunha Marinho[2], C.L. Da Silva[74],
E. Dall'Occo[27], J. Dalseno[48], A. Danilina[34], A. Davis[3], O. De Aguiar Francisco[42], K. De Bruyn[42],
S. De Capua[56], M. De Cian[43], J.M. De Miranda[1], L. De Paula[2], M. De Serio[14,d], P. De Simone[18],
C.T. Dean[53], D. Decamp[4], L. Del Buono[8], B. Delaney[49], H.-P. Dembinski[11], M. Demmer[10],
A. Dendek[30], D. Derkach[37], O. Deschamps[5], F. Desse[7], F. Dettori[54], B. Dey[65], A. Di Canto[42],
P. Di Nezza[18], S. Didenko[70], H. Dijkstra[42], F. Dordei[42], M. Dorigo[42,y], A. Dosil Suárez[41],
L. Douglas[53], A. Dovbnya[45], K. Dreimanis[54], L. Dufour[27], G. Dujany[8], P. Durante[42],
J.M. Durham[74], D. Dutta[56], R. Dzhelyadin[39], M. Dziewiecki[12], A. Dziurda[29], A. Dzyuba[33],
S. Easo[51], U. Egede[55], V. Egorychev[34], S. Eidelman[38,w], S. Eisenhardt[52], U. Eitschberger[10],
R. Ekelhof[10], L. Eklund[53], S. Ely[61], A. Ene[32], S. Escher[9], S. Esen[27], T. Evans[59], A. Falabella[15],
N. Farley[47], S. Farry[54], D. Fazzini[20,42,i], L. Federici[25], G. Fernandez[40], P. Fernandez Declara[42],
A. Fernandez Prieto[41], F. Ferrari[15], L. Ferreira Lopes[43], F. Ferreira Rodrigues[2], M. Ferro-Luzzi[42],
S. Filippov[36], R.A. Fini[14], M. Fiorini[16,g], M. Firlej[30], C. Fitzpatrick[43], T. Fiutowski[30],
F. Fleuret[7,b], M. Fontana[22,42], F. Fontanelli[19,h], R. Forty[42], V. Franco Lima[54], M. Frank[42],
C. Frei[42], J. Fu[21,q], W. Funk[42], C. Färber[42], M. Féo Pereira Rivello Carvalho[27], E. Gabriel[52],
A. Gallas Torreira[41], D. Galli[15,e], S. Gallorini[23], S. Gambetta[52], M. Gandelman[2], P. Gandini[21],
Y. Gao[3], L.M. Garcia Martin[72], B. Garcia Plana[41], J. García Pardiñas[44], J. Garra Tico[49],
L. Garrido[40], D. Gascon[40], C. Gaspar[42], L. Gavardi[10], G. Gazzoni[5], D. Gerick[12], E. Gersabeck[56],
M. Gersabeck[56], T. Gershon[50], D. Gerstel[6], Ph. Ghez[4], S. Gianì[43], V. Gibson[49], O.G. Girard[43],

L. Giubega[32], K. Gizdov[52], V.V. Gligorov[8], D. Golubkov[34], A. Golutvin[55,70], A. Gomes[1,a],
I.V. Gorelov[35], C. Gotti[20,i], E. Govorkova[27], J.P. Grabowski[12], R. Graciani Diaz[40],
L.A. Granado Cardoso[42], E. Graugés[40], E. Graverini[44], G. Graziani[17], A. Grecu[32], R. Greim[27],
P. Griffith[22], L. Grillo[56], L. Gruber[42], B.R. Gruberg Cazon[57], O. Grünberg[67], C. Gu[3],
E. Gushchin[36], Yu. Guz[39,42], T. Gys[42], C. Göbel[62], T. Hadavizadeh[57], C. Hadjivasiliou[5],
G. Haefeli[43], C. Haen[42], S.C. Haines[49], B. Hamilton[60], X. Han[12], T.H. Hancock[57],
S. Hansmann-Menzemer[12], N. Harnew[57], S.T. Harnew[48], T. Harrison[54], C. Hasse[42], M. Hatch[42],
J. He[63], M. Hecker[55], K. Heinicke[10], A. Heister[9], K. Hennessy[54], L. Henry[72], E. van Herwijnen[42],
M. Heß[67], A. Hicheur[2], D. Hill[57], M. Hilton[56], P.H. Hopchev[43], W. Hu[65], W. Huang[63],
Z.C. Huard[59], W. Hulsbergen[27], T. Humair[55], M. Hushchyn[37], D. Hutchcroft[54], D. Hynds[27],
P. Ibis[10], M. Idzik[30], P. Ilten[47], K. Ivshin[33], R. Jacobsson[42], J. Jalocha[57], E. Jans[27],
A. Jawahery[60], F. Jiang[3], M. John[57], D. Johnson[42], C.R. Jones[49], C. Joram[42], B. Jost[42],
N. Jurik[57], S. Kandybei[45], M. Karacson[42], J.M. Kariuki[48], S. Karodia[53], N. Kazeev[37],
M. Kecke[12], F. Keizer[49], M. Kelsey[61], M. Kenzie[49], T. Ketel[28], E. Khairullin[37], B. Khanji[12],
C. Khurewathanakul[43], K.E. Kim[61], T. Kirn[9], S. Klaver[18], K. Klimaszewski[31], T. Klimkovich[11],
S. Koliiev[46], M. Kolpin[12], R. Kopecna[12], P. Koppenburg[27], I. Kostiuk[27], S. Kotriakhova[33],
M. Kozeiha[5], L. Kravchuk[36], M. Kreps[50], F. Kress[55], P. Krokovny[38,w], W. Krupa[30],
W. Krzemien[31], W. Kucewicz[29,l], M. Kucharczyk[29], V. Kudryavtsev[38,w], A.K. Kuonen[43],
T. Kvaratskheliya[34,42], D. Lacarrere[42], G. Lafferty[56], A. Lai[22], D. Lancierini[44], G. Lanfranchi[18],
C. Langenbruch[9], T. Latham[50], C. Lazzeroni[47], R. Le Gac[6], A. Leflat[35], J. Lefrançois[7],
R. Lefévre[5], F. Lemaitre[42], O. Leroy[6], T. Lesiak[29], B. Leverington[12], P.-R. Li[63], T. Li[3], Z. Li[61],
X. Liang[61], T. Likhomanenko[69], R. Lindner[42], F. Lionetto[44], V. Lisovskyi[7], X. Liu[3], D. Loh[50],
A. Loi[22], I. Longstaff[53], J.H. Lopes[2], G.H. Lovell[49], D. Lucchesi[23,o], M. Lucio Martinez[41],
A. Lupato[23], E. Luppi[16,g], O. Lupton[42], A. Lusiani[24], X. Lyu[63], F. Machefert[7], F. Maciuc[32],
V. Macko[43], P. Mackowiak[10], S. Maddrell-Mander[48], O. Maev[33,42], K. Maguire[56],
D. Maisuzenko[33], M.W. Majewski[30], S. Malde[57], B. Malecki[29], A. Malinin[69], T. Maltsev[38,w],
G. Manca[22,f], G. Mancinelli[6], D. Marangotto[21,q], J. Maratas[5,v], J.F. Marchand[4], U. Marconi[15],
C. Marin Benito[40], M. Marinangeli[43], P. Marino[43], J. Marks[12], G. Martellotti[26], M. Martin[6],
M. Martinelli[42], D. Martinez Santos[41], F. Martinez Vidal[72], A. Massafferri[1], R. Matev[42],
A. Mathad[50], Z. Mathe[42], C. Matteuzzi[20], A. Mauri[44], E. Maurice[7,b], B. Maurin[43], A. Mazurov[47],
M. McCann[55,42], A. McNab[56], R. McNulty[13], J.V. Mead[54], B. Meadows[59], C. Meaux[6],
F. Meier[10], N. Meinert[67], D. Melnychuk[31], M. Merk[27], A. Merli[21,q], E. Michielin[23],
D.A. Milanes[66], E. Millard[50], M.-N. Minard[4], L. Minzoni[16,g], D.S. Mitzel[12], A. Mogini[8],
J. Molina Rodriguez[1,z], T. Mombächer[10], I.A. Monroy[66], S. Monteil[5], M. Morandin[23],
G. Morello[18], M.J. Morello[24,t], O. Morgunova[69], J. Moron[30], A.B. Morris[6], R. Mountain[61],
F. Muheim[52], M. Mulder[27], C.H. Murphy[57], D. Murray[56], D. Müller[42], J. Müller[10], K. Müller[44],
V. Müller[10], P. Naik[48], T. Nakada[43], R. Nandakumar[51], A. Nandi[57], T. Nanut[43], I. Nasteva[2],
M. Needham[52], N. Neri[21], S. Neubert[12], N. Neufeld[42], M. Neuner[12], T.D. Nguyen[43],
C. Nguyen-Mau[43,n], S. Nieswand[9], R. Niet[10], N. Nikitin[35], A. Nogay[69], D.P. O'Hanlon[15],
A. Oblakowska-Mucha[30], V. Obraztsov[39], S. Ogilvy[18], R. Oldeman[22,f], C.J.G. Onderwater[68],
A. Ossowska[29], J.M. Otalora Goicochea[2], P. Owen[44], A. Oyanguren[72], P.R. Pais[43], A. Palano[14],
M. Palutan[18,42], G. Panshin[71], A. Papanestis[51], M. Pappagallo[52], L.L. Pappalardo[16,g],
W. Parker[60], C. Parkes[56], G. Passaleva[17,42], A. Pastore[14], M. Patel[55], C. Patrignani[15,e],
A. Pearce[42], A. Pellegrino[27], G. Penso[26], M. Pepe Altarelli[42], S. Perazzini[42], D. Pereima[34],
P. Perret[5], L. Pescatore[43], K. Petridis[48], A. Petrolini[19,h], A. Petrov[69], S. Petrucci[52],
M. Petruzzo[21,q], B. Pietrzyk[4], G. Pietrzyk[43], M. Pikies[29], M. Pili[57], D. Pinci[26], J. Pinzino[42],
F. Pisani[42], A. Piucci[12], V. Placinta[32], S. Playfer[52], J. Plews[47], M. Plo Casasus[41], F. Polci[8],
M. Poli Lener[18], A. Poluektov[50], N. Polukhina[70,c], I. Polyakov[61], E. Polycarpo[2], G.J. Pomery[48],

S. Ponce[42], A. Popov[39], D. Popov[47,11], S. Poslavskii[39], C. Potterat[2], E. Price[48], J. Prisciandaro[41],
C. Prouve[48], V. Pugatch[46], A. Puig Navarro[44], H. Pullen[57], G. Punzi[24,p], W. Qian[63], J. Qin[63],
R. Quagliani[8], B. Quintana[5], B. Rachwal[30], J.H. Rademacker[48], M. Rama[24], M. Ramos Pernas[41],
M.S. Rangel[2], F. Ratnikov[37,x], G. Raven[28], M. Ravonel Salzgeber[42], M. Reboud[4], F. Redi[43],
S. Reichert[10], A.C. dos Reis[1], F. Reiss[8], C. Remon Alepuz[72], Z. Ren[3], V. Renaudin[7],
S. Ricciardi[51], S. Richards[48], K. Rinnert[54], P. Robbe[7], A. Robert[8], A.B. Rodrigues[43],
E. Rodrigues[59], J.A. Rodriguez Lopez[66], M. Roehrken[42], A. Rogozhnikov[37], S. Roiser[42],
A. Rollings[57], V. Romanovskiy[39], A. Romero Vidal[41], M. Rotondo[18], M.S. Rudolph[61], T. Ruf[42],
J. Ruiz Vidal[72], J.J. Saborido Silva[41], N. Sagidova[33], B. Saitta[22,f], V. Salustino Guimaraes[62],
C. Sanchez Gras[27], C. Sanchez Mayordomo[72], B. Sanmartin Sedes[41], R. Santacesaria[26],
C. Santamarina Rios[41], M. Santimaria[18], E. Santovetti[25,j], G. Sarpis[56], A. Sarti[18,k],
C. Satriano[26,s], A. Satta[25], M. Saur[63], D. Savrina[34,35], S. Schael[9], M. Schellenberg[10],
M. Schiller[53], H. Schindler[42], M. Schmelling[11], T. Schmelzer[10], B. Schmidt[42], O. Schneider[43],
A. Schopper[42], H.F. Schreiner[59], M. Schubiger[43], M.H. Schune[7], R. Schwemmer[42], B. Sciascia[18],
A. Sciubba[26,k], A. Semennikov[34], E.S. Sepulveda[8], A. Sergi[47,42], N. Serra[44], J. Serrano[6],
L. Sestini[23], P. Seyfert[42], M. Shapkin[39], Y. Shcheglov[33,†], T. Shears[54], L. Shekhtman[38,w],
V. Shevchenko[69], E. Shmanin[70], B.G. Siddi[16], R. Silva Coutinho[44], L. Silva de Oliveira[2],
G. Simi[23,o], S. Simone[14,d], N. Skidmore[12], T. Skwarnicki[61], J.G. Smeaton[49], E. Smith[9],
I.T. Smith[52], M. Smith[55], M. Soares[15], l. Soares Lavra[1], M.D. Sokoloff[59], F.J.P. Soler[53],
B. Souza De Paula[2], B. Spaan[10], P. Spradlin[53], F. Stagni[42], M. Stahl[12], S. Stahl[42], P. Stefko[43],
S. Stefkova[55], O. Steinkamp[44], S. Stemmle[12], O. Stenyakin[39], M. Stepanova[33], H. Stevens[10],
S. Stone[61], B. Storaci[44], S. Stracka[24,p], M.E. Stramaglia[43], M. Straticiuc[32], U. Straumann[44],
S. Strokov[71], J. Sun[3], L. Sun[64], K. Swientek[30], V. Syropoulos[28], T. Szumlak[30], M. Szymanski[63],
S. T'Jampens[4], Z. Tang[3], A. Tayduganov[6], T. Tekampe[10], G. Tellarini[16], F. Teubert[42],
E. Thomas[42], J. van Tilburg[27], M.J. Tilley[55], V. Tisserand[5], S. Tolk[42], L. Tomassetti[16,g],
D. Tonelli[24], D.Y. Tou[8], R. Tourinho Jadallah Aoude[1], E. Tournefier[4], S. Tourneur[43], M. Traill[53],
M.T. Tran[43], A. Trisovic[49], A. Tsaregorodtsev[6], A. Tully[49], N. Tuning[27,42], A. Ukleja[31],
A. Usachov[7], A. Ustyuzhanin[37], U. Uwer[12], C. Vacca[22,f], A. Vagner[71], V. Vagnoni[15], A. Valassi[42],
S. Valat[42], G. Valenti[15], R. Vazquez Gomez[42], P. Vazquez Regueiro[41], S. Vecchi[16],
M. van Veghel[27], J.J. Velthuis[48], M. Veltri[17,r], G. Veneziano[57], A. Venkateswaran[61],
T.A. Verlage[9], M. Vernet[5], M. Vesterinen[57], J.V. Viana Barbosa[42], D. Vieira[63],
M. Vieites Diaz[41], H. Viemann[67], X. Vilasis-Cardona[40,m], A. Vitkovskiy[27], M. Vitti[49],
V. Volkov[35], A. Vollhardt[44], B. Voneki[42], A. Vorobyev[33], V. Vorobyev[38,w], J.A. de Vries[27],
C. Vázquez Sierra[27], R. Waldi[67], J. Walsh[24], J. Wang[61], M. Wang[3], Y. Wang[65], Z. Wang[44],
D.R. Ward[49], H.M. Wark[54], N.K. Watson[47], D. Websdale[55], A. Weiden[44], C. Weisser[58],
M. Whitehead[9], J. Wicht[50], G. Wilkinson[57], M. Wilkinson[61], I. Williams[49], M.R.J. Williams[56],
M. Williams[58], T. Williams[47], F.F. Wilson[51,42], J. Wimberley[60], J. Winn[7], J. Wishahi[10],
W. Wislicki[31], M. Witek[29], G. Wormser[7], S.A. Wotton[49], K. Wyllie[42], D. Xiao[65], Y. Xie[65],
A. Xu[3], M. Xu[65], Q. Xu[63], Z. Xu[3], Z. Xu[4], Z. Yang[3], Z. Yang[60], Y. Yao[61], L.E. Yeomans[54],
H. Yin[65], J. Yu[65,ab], X. Yuan[61], O. Yushchenko[39], K.A. Zarebski[47], M. Zavertyaev[11,c],
D. Zhang[65], L. Zhang[3], W.C. Zhang[3,aa], Y. Zhang[7], A. Zhelezov[12], Y. Zheng[63], X. Zhu[3],
V. Zhukov[9,35], J.B. Zonneveld[52], S. Zucchelli[15]

1   Centro Brasileiro de Pesquisas Físicas (CBPF), Rio de Janeiro, Brazil
2   Universidade Federal do Rio de Janeiro (UFRJ), Rio de Janeiro, Brazil
3   Center for High Energy Physics, Tsinghua University, Beijing, China
4   Univ. Grenoble Alpes, Univ. Savoie Mont Blanc, CNRS, IN2P3-LAPP, Annecy, France
5   Clermont Université, Université Blaise Pascal, CNRS/IN2P3, LPC, Clermont-Ferrand, France
6   Aix Marseille Université, CNRS/IN2P3, CPPM, Marseille, France

[7] *LAL, Université Paris-Sud, CNRS/IN2P3, Université Paris-Saclay, Orsay, France*

[8] *LPNHE, Sorbonne Université, Paris Diderot Sorbonne Paris Cité, CNRS/IN2P3, Paris, France*

[9] *I. Physikalisches Institut, RWTH Aachen University, Aachen, Germany*

[10] *Fakultät Physik, Technische Universität Dortmund, Dortmund, Germany*

[11] *Max-Planck-Institut für Kernphysik (MPIK), Heidelberg, Germany*

[12] *Physikalisches Institut, Ruprecht-Karls-Universität Heidelberg, Heidelberg, Germany*

[13] *School of Physics, University College Dublin, Dublin, Ireland*

[14] *INFN Sezione di Bari, Bari, Italy*

[15] *INFN Sezione di Bologna, Bologna, Italy*

[16] *INFN Sezione di Ferrara, Ferrara, Italy*

[17] *INFN Sezione di Firenze, Firenze, Italy*

[18] *INFN Laboratori Nazionali di Frascati, Frascati, Italy*

[19] *INFN Sezione di Genova, Genova, Italy*

[20] *INFN Sezione di Milano-Bicocca, Milano, Italy*

[21] *INFN Sezione di Milano, Milano, Italy*

[22] *INFN Sezione di Cagliari, Monserrato, Italy*

[23] *INFN Sezione di Padova, Padova, Italy*

[24] *INFN Sezione di Pisa, Pisa, Italy*

[25] *INFN Sezione di Roma Tor Vergata, Roma, Italy*

[26] *INFN Sezione di Roma La Sapienza, Roma, Italy*

[27] *Nikhef National Institute for Subatomic Physics, Amsterdam, Netherlands*

[28] *Nikhef National Institute for Subatomic Physics and VU University Amsterdam, Amsterdam, Netherlands*

[29] *Henryk Niewodniczanski Institute of Nuclear Physics Polish Academy of Sciences, Kraków, Poland*

[30] *AGH — University of Science and Technology, Faculty of Physics and Applied Computer Science, Kraków, Poland*

[31] *National Center for Nuclear Research (NCBJ), Warsaw, Poland*

[32] *Horia Hulubei National Institute of Physics and Nuclear Engineering, Bucharest-Magurele, Romania*

[33] *Petersburg Nuclear Physics Institute (PNPI), Gatchina, Russia*

[34] *Institute of Theoretical and Experimental Physics (ITEP), Moscow, Russia*

[35] *Institute of Nuclear Physics, Moscow State University (SINP MSU), Moscow, Russia*

[36] *Institute for Nuclear Research of the Russian Academy of Sciences (INR RAS), Moscow, Russia*

[37] *Yandex School of Data Analysis, Moscow, Russia*

[38] *Budker Institute of Nuclear Physics (SB RAS), Novosibirsk, Russia*

[39] *Institute for High Energy Physics (IHEP), Protvino, Russia*

[40] *ICCUB, Universitat de Barcelona, Barcelona, Spain*

[41] *Instituto Galego de Física de Altas Enerxías (IGFAE), Universidade de Santiago de Compostela, Santiago de Compostela, Spain*

[42] *European Organization for Nuclear Research (CERN), Geneva, Switzerland*

[43] *Institute of Physics, Ecole Polytechnique Fédérale de Lausanne (EPFL), Lausanne, Switzerland*

[44] *Physik-Institut, Universität Zürich, Zürich, Switzerland*

[45] *NSC Kharkiv Institute of Physics and Technology (NSC KIPT), Kharkiv, Ukraine*

[46] *Institute for Nuclear Research of the National Academy of Sciences (KINR), Kyiv, Ukraine*

[47] *University of Birmingham, Birmingham, United Kingdom*

[48] *H.H. Wills Physics Laboratory, University of Bristol, Bristol, United Kingdom*

[49] *Cavendish Laboratory, University of Cambridge, Cambridge, United Kingdom*

[50] *Department of Physics, University of Warwick, Coventry, United Kingdom*

[51] *STFC Rutherford Appleton Laboratory, Didcot, United Kingdom*

[52] *School of Physics and Astronomy, University of Edinburgh, Edinburgh, United Kingdom*

[53] *School of Physics and Astronomy, University of Glasgow, Glasgow, United Kingdom*

[54] *Oliver Lodge Laboratory, University of Liverpool, Liverpool, United Kingdom*

[55] *Imperial College London, London, United Kingdom*

[56] *School of Physics and Astronomy, University of Manchester, Manchester, United Kingdom*

[57] *Department of Physics, University of Oxford, Oxford, United Kingdom*

[58] *Massachusetts Institute of Technology, Cambridge, MA, United States*

[59] *University of Cincinnati, Cincinnati, OH, United States*

[60] *University of Maryland, College Park, MD, United States*

[61] *Syracuse University, Syracuse, NY, United States*

[62] *Pontifícia Universidade Católica do Rio de Janeiro (PUC-Rio), Rio de Janeiro, Brazil, associated to [2]*

[63] *University of Chinese Academy of Sciences, Beijing, China, associated to [3]*

[64] *School of Physics and Technology, Wuhan University, Wuhan, China, associated to [3]*

[65] *Institute of Particle Physics, Central China Normal University, Wuhan, Hubei, China, associated to [3]*

[66] *Departamento de Fisica, Universidad Nacional de Colombia, Bogota, Colombia, associated to [8]*

[67] *Institut für Physik, Universität Rostock, Rostock, Germany, associated to [12]*

[68] *Van Swinderen Institute, University of Groningen, Groningen, Netherlands, associated to [27]*

[69] *National Research Centre Kurchatov Institute, Moscow, Russia, associated to [34]*

[70] *National University of Science and Technology "MISIS", Moscow, Russia, associated to [34]*

[71] *National Research Tomsk Polytechnic University, Tomsk, Russia, associated to [34]*

[72] *Instituto de Fisica Corpuscular, Centro Mixto Universidad de Valencia — CSIC, Valencia, Spain, associated to [40]*

[73] *University of Michigan, Ann Arbor, United States, associated to [61]*

[74] *Los Alamos National Laboratory (LANL), Los Alamos, United States, associated to [61]*

[a] *Universidade Federal do Triângulo Mineiro (UFTM), Uberaba-MG, Brazil*

[b] *Laboratoire Leprince-Ringuet, Palaiseau, France*

[c] *P.N. Lebedev Physical Institute, Russian Academy of Science (LPI RAS), Moscow, Russia*

[d] *Università di Bari, Bari, Italy*

[e] *Università di Bologna, Bologna, Italy*

[f] *Università di Cagliari, Cagliari, Italy*

[g] *Università di Ferrara, Ferrara, Italy*

[h] *Università di Genova, Genova, Italy*

[i] *Università di Milano Bicocca, Milano, Italy*

[j] *Università di Roma Tor Vergata, Roma, Italy*

[k] *Università di Roma La Sapienza, Roma, Italy*

[l] *AGH — University of Science and Technology, Faculty of Computer Science, Electronics and Telecommunications, Kraków, Poland*

[m] *LIFAELS, La Salle, Universitat Ramon Llull, Barcelona, Spain*

[n] *Hanoi University of Science, Hanoi, Vietnam*

[o] *Università di Padova, Padova, Italy*

[p] *Università di Pisa, Pisa, Italy*

[q] *Università degli Studi di Milano, Milano, Italy*

[r] *Università di Urbino, Urbino, Italy*

[s] *Università della Basilicata, Potenza, Italy*

[t] *Scuola Normale Superiore, Pisa, Italy*

[u] *Università di Modena e Reggio Emilia, Modena, Italy*

[v] *MSU — Iligan Institute of Technology (MSU-IIT), Iligan, Philippines*

[w] *Novosibirsk State University, Novosibirsk, Russia*

[x] *National Research University Higher School of Economics, Moscow, Russia*

[y] *Sezione INFN di Trieste, Trieste, Italy*

[z] *Escuela Agrícola Panamericana, San Antonio de Oriente, Honduras*

[aa] *School of Physics and Information Technology, Shaanxi Normal University (SNNU), Xi'an, China*

[ab] *Physics and Micro Electronic College, Hunan University, Changsha City, China*

[†] *Deceased*